AD-A114 250 MATHEMATICAL SCIENCES NORTHWEST INC BELLEVUE WA F/G 20/5
ATTENUATION OF LARGE AMPLITUDE PRESSURE DISTURBANCES BY LIQUID --ETC(U)
DEC 81 W J THAYER, E L KLOSTERMAN F49620-80-C-0094
UNCLASSIFIED AFOSR-TR-82-0344 NL

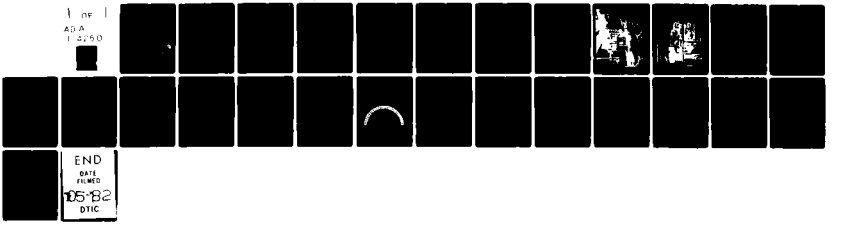

END
DATE FILMED
05-82
DTIC

(5)

ATTENUATION OF LARGE AMPLITUDE PRESSURE DISTURBANCES BY LIQUID DROPLETS

Annual Report
30 September 1980 - 30 September 1981

Contract No. F49620-80-C-0094

Submitted To
Air Force Office of Scientific Research
Bolling Air Force Base, D.C. 20332

By
Mathematical Sciences Northwest, Inc.
Bellevue, Washington 98004

14 December 1981

UNCLASSIFIED

SECURITY CLASSIFICATION OF THIS PAGE (When Data Entered)

REPORT DOCUMENTATION PAGE		READ INSTRUCTIONS BEFORE COMPLETING FORM
1. REPORT NUMBER AFOSR-TR- 82-0344	2. GOVT ACCESSION NO. AD-A114 250	3. RECIPIENT'S CATALOG NUMBER
4. TITLE (and Subtitle) ATTENUATION OF LARGE AMPLITUDE PRESSURE DISTURBANCES BY LIQUID DROPLETS		5. TYPE OF REPORT & PERIOD COVERED ANNUAL REPORT Sept 1980 - 30 Sept 1981 6. PERFORMING ORG. REPORT NUMBER
7. AUTHOR(s) WILLIAM J. THAYER III and E. LEE KLOSTERMAN		8. CONTRACT OR GRANT NUMBER(s) F49620-80-C-0094
9. PERFORMING ORGANIZATION NAME AND ADDRESS MATHEMATICAL SCIENCES NORTHWEST, INC. 2755 Northup Way Bellevue, Washington 98004		10. PROGRAM ELEMENT, PROJECT, TASK AREA & WORK UNIT NUMBERS 61102F 2307/A4
11. CONTROLLING OFFICE NAME AND ADDRESS Air Force Office of Scientific Research/NA Building 410 Bolling Air Force Base, D.C. 20332		12. REPORT DATE 14 December 1981 13. NUMBER OF PAGES 24
14. MONITORING AGENCY NAME & ADDRESS(if different from Controlling Office)		15. SECURITY CLASS. (of this report) Unclassified 15a. DECLASSIFICATION/DOWNGRADING SCHEDULE
16. DISTRIBUTION STATEMENT (of this Report) Approved for public release; distribution unlimited.		
17. DISTRIBUTION STATEMENT (of the abstract entered in Block 20, if different from Report)		
18. SUPPLEMENTARY NOTES		
19. KEY WORDS (Continue on reverse side if necessary and identify by block number) Droplets Pressure Wave Suppression Shock Tubes Light Scattering Pulsed Lasers		
20. ABSTRACT (Continue on reverse side if necessary and identify by block number) This report summarizes activities carried out to investigate flow processes which govern the attenuation of large amplitude pressure disturbances in gases containing high mass fractions of liquid droplets. A shock tube driver and steady flow test section with supporting gas and liquid supplies, control, and monitoring instruments have been developed for tests. The test regime includes droplet/gas mass ratios from 0.1 to 1.0, shock pressure ratios up to 5.6, and initial gas and liquid temperatures from ambient to 98 C. An optical diagnostic		

DD FORM 1 JAN 73 1473 EDITION OF 1 NOV 65 IS OBSOLETE

UNCLASSIFIED

SECURITY CLASSIFICATION OF THIS PAGE (When Data Entered)

system has been developed to determine the dynamic response of the droplet field to rapidly varying flows behind shock waves. The angular distribution of scattered light from a probe laser beam is monitored using a photodetector array and associated high frequency response data acquisition equipment. Data for a complete size distribution measurement is acquired and stored every 40 μsec. The droplet size distributions and number of densities are determined from the scattered and attenuated light measurements using a data reduction code based on scattering theory. The pressure wave amplitude and waveform is determined as a function of location and time using high frequency response pressure transducers. The test apparatus and diagnostic system were developed to the point of checkout testing during the first year of the program. Wave attenuation and droplet dynamics testing will begin early in the second program year.

Section 1

INTRODUCTION

Dense fields of liquid droplets may provide unique advantages over alternative techniques for suppressing or attenuating shock waves and other strong pressure disturbances for pulsed laser acoustic attenuation. The rapid transfer of momentum, energy, and mass between gas, vapor, and liquid species in regions of rapid pressure, velocity, and temperature fluctuations can quickly suppress large amplitude pressure disturbances. In addition, the presence of liquid droplets in the region immediately downstream of the laser cavity makes possible the rapid homogenization of hot/cold gas interfaces which could otherwise reflect disturbances into the cavity region. By controlling the droplet injection rates, locations, droplet sizes, and duct configuration, a droplet attenuator duct can be "tuned" to minimize pressure disturbances and maximize medium uniformity in a laser cavity. The liquid species can also be used to chemically scrub the laser effluent stream to remove hazardous materials.

Attenuation of 3 to 10 atm pressure disturbances by three orders of magnitude has been demonstrated within 1 to 5 msec of reaction pulses in a pulsed chemical laser device utilizing water spray attenuation.[1] This was an order of magnitude better than was achieved in early work using the more conventional techniques of bulk absorbers in the flow channel, perforated duct mufflers, or broadband Helmholtz resonators along the flow boundaries.

Research has been carried out to study the effects of attenuator duct configuration and droplet size on droplet acoustic suppressor performance.[2] This work has allowed some optimization of the spray wave attenuator technique prior to its application to a larger scale, repetitively pulsed laser development program. However, the basic processes which govern spray attenuator performance are not yet well characterized either experimentally or analytically. Better

characterization would allow optimization of droplet acoustic attenuator operation with respect to total liquid flow requirements, droplet size and number distribution, and response to a range of pulsed laser conditions. Such an understanding could allow this technique to be applied with other liquids to alternate high power pulsed lasers operating at visible or shorter wavelengths where more attenuation is required than appears feasible using dry, conventional attenuators.

Development of droplet attenuation techniques is currently hindered by a lack of experimental data and analytical models for propagation and attenuation of strong pressure disturbances through gases containing large numbers of liquid droplets. Current understanding of the attenuation of strong pressure waves by liquid droplets contained within the disturbed gas volume is limited to 1) knowledge of the stability and dynamic behavior of single droplets in unsteady flow, and 2) knowledge of very low amplitude (acoustic) pressure wave attenuation by droplets in air/droplet mixtures having low droplet number densities and liquid mass fractions (less than 1 percent of the gas mass). Considerable experimental work has been conducted on the interaction of shock-induced flows with individual droplets.[3,4] Sufficient experimental work has been done to characterize single droplet dynamics by separate regimes where viscous drag, droplet deformation, droplet stripping, or gross instability with consequent shattering dominate. However, this experimental work was directed at understanding sources of re-entry vehicle erosion in situations where droplet number densities were very low, droplets could be assumed to act individually, and the droplet dynamics could safely be assumed to have negligible effect on the mean gas flow. The literature contains no experimental data and only suggestions for analysis[5,6] of the attenuation of shock waves by liquid droplets. Separate literature deals with the attenuation of low amplitude acoustic disturbances by very low number droplet/gas mixtures.[7,8] In this regime, droplet deformation and breakup do not occur, droplet collisions and agglomeration are negligible, and linear equations adequately describe the phenomena governing attenuation of acoustic waves. This earlier work has been directed at

gas/droplet mixtures in which droplets represent a mass fraction of one percent of the gas or less. Propagation and attenuation of strong pressure waves in dense sprays has received very little consideration. The present program is primarily directed at experimentally investigating this important regime.

The specific objective of the present program is to characterize the dynamics of dense droplet fields (mass of droplets per unit gas volume comparable to the gas density) in rapidly accelerated flows. The principal new phenomena that arise when considering dense droplet fields are associated with the close proximity and consequent strong interactions between neighboring droplets. Phenomena which require study are:

1) Fluid dynamics interactions of various size droplets as affected by acceleration, deformation, and shattering of nearby dropets of similar or dissimilar sizes;

2) Agglomeration of droplets of various sizes as affected by relative response times of nearby droplets to flow disturbances; and

3) Energy and mass transport between the gas stream and vaporizing (condensing) droplets in the presence of nearby droplets.

Analytical and empirical models which adequately represent these processes for a large droplet size range, high droplet density, and large pressure wave amplitudes will be developed and experimentally confirmed. This information will provide the foundation for accurate predictions of pressure wave suppression by the use of dense liquid sprays.

Section 2

SHOCK TUBE TEST APPARATUS

The apparatus which will be used for pressure wave attenuation and droplet dynamics experiments consists of a test section filled with a droplet/air mixture and a shock tube driver to generate large amplitude pressure waves. A schematic diagram of the test apparatus is shown in Figure 1. Many components are shown in Figure 1 in addition to the shock tube driver and driven sections. These additional components are required for establishing test conditions in the test (or driven) section, for taking data, etc. The test apparatus has been installed in the laboratory, and plumbing and electrical work are essentially complete. Photographs of the test apparatus are presented in Figures 2 and 3 during the installation of the injector plumbing. Various features of the test apparatus and its operation are described below.

An existing 5 inch square shock tube has been used for the test apparatus. The driver section is currently ~2.4 meters (8 feet) long but can be extended to 4.8 meters by using an existing extra section. This driver section can be operated at up to 150 psi pressure and will be used to generate a range of shock wave pressure ratios in the droplet/gas mixtures. For operation with a helium/argon driver gas which is tailored to prevent wave reflections from the driven gas interface, shock pressure ratios P_2/P_1 of up to 2.7 will be provided. Stronger waves, i.e., pressure ratios up to 5.5, will be provided by using helium to generate the shock wave in the air/droplet test medium. The 4.9 meter long test section will be operated at ambient initial pressure with the droplet/gas mixture flowing through it. The shock tube is attached to a massive thrust block at the interface between the driver and test sections to minimize shock-induced vibrations and movement of the test section during data acquisition. A double diaphragm arrangement is being used to accurately control test conditions and the time of diaphragm burst. In this technique, the pressure difference between the shock tube driver and

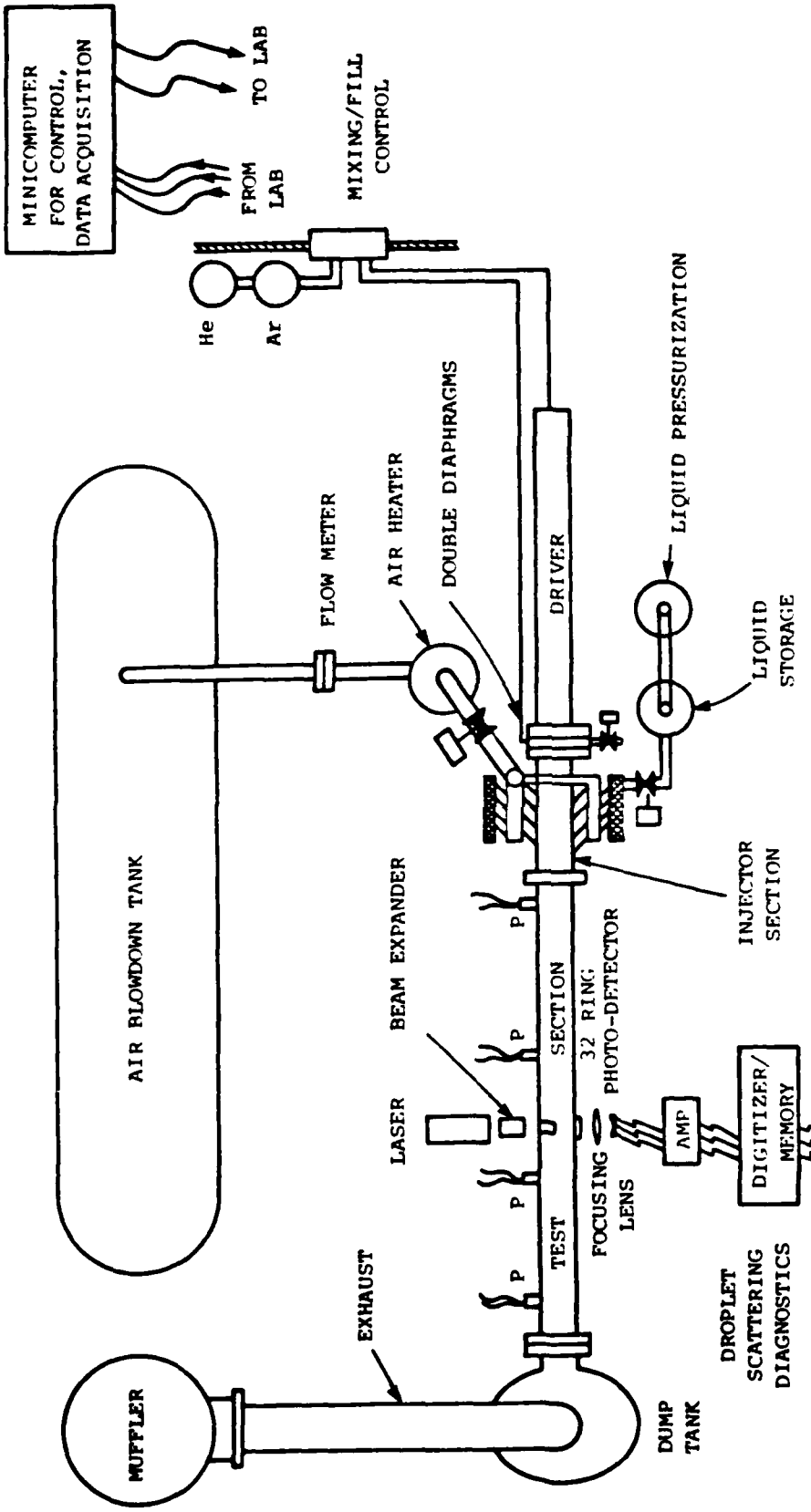

Figure 1. Schematic Diagram of Spray Attenuation Test Apparatus.

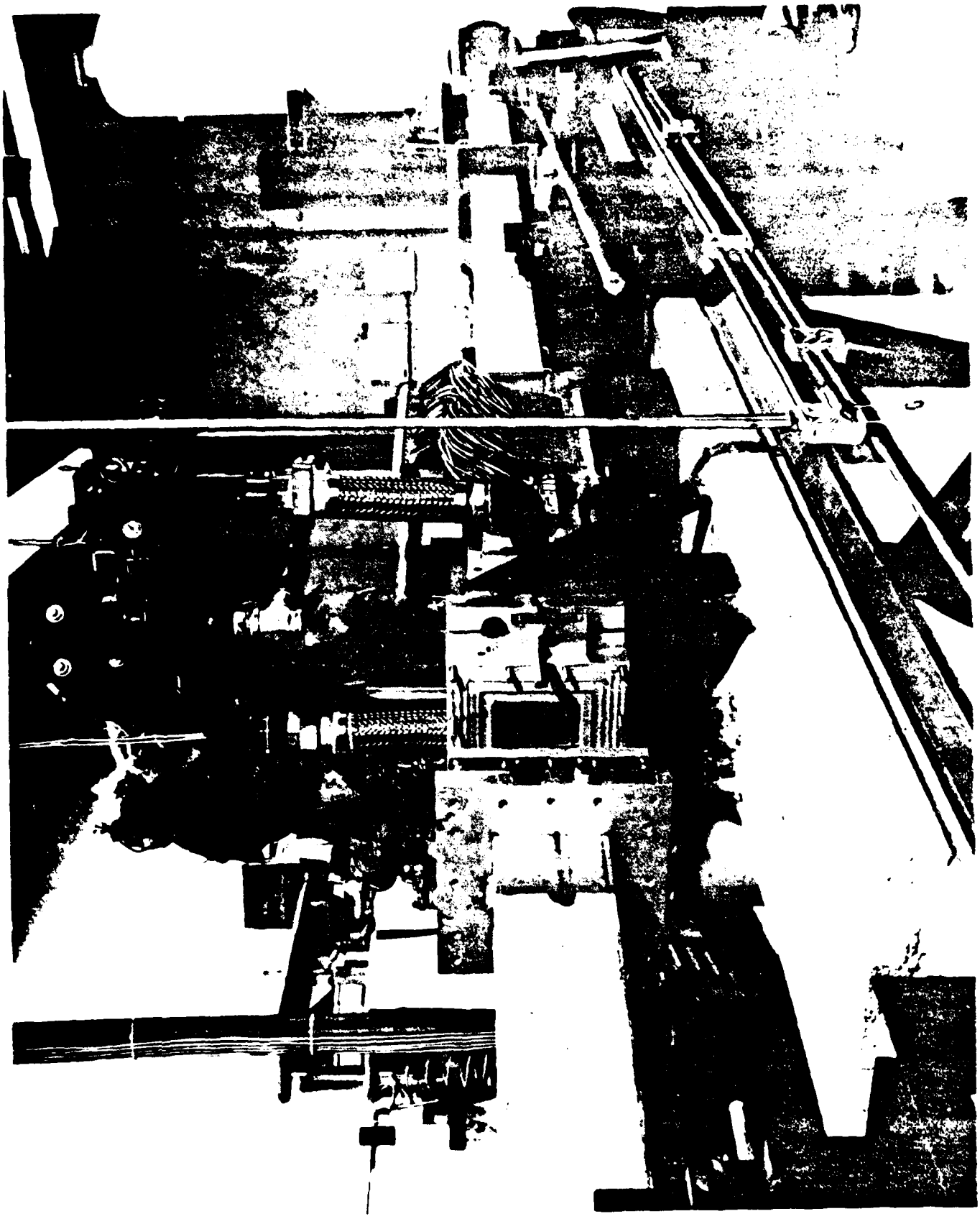

Figure 2. Shock Tube Test Apparatus with Supply and Control Flow System.

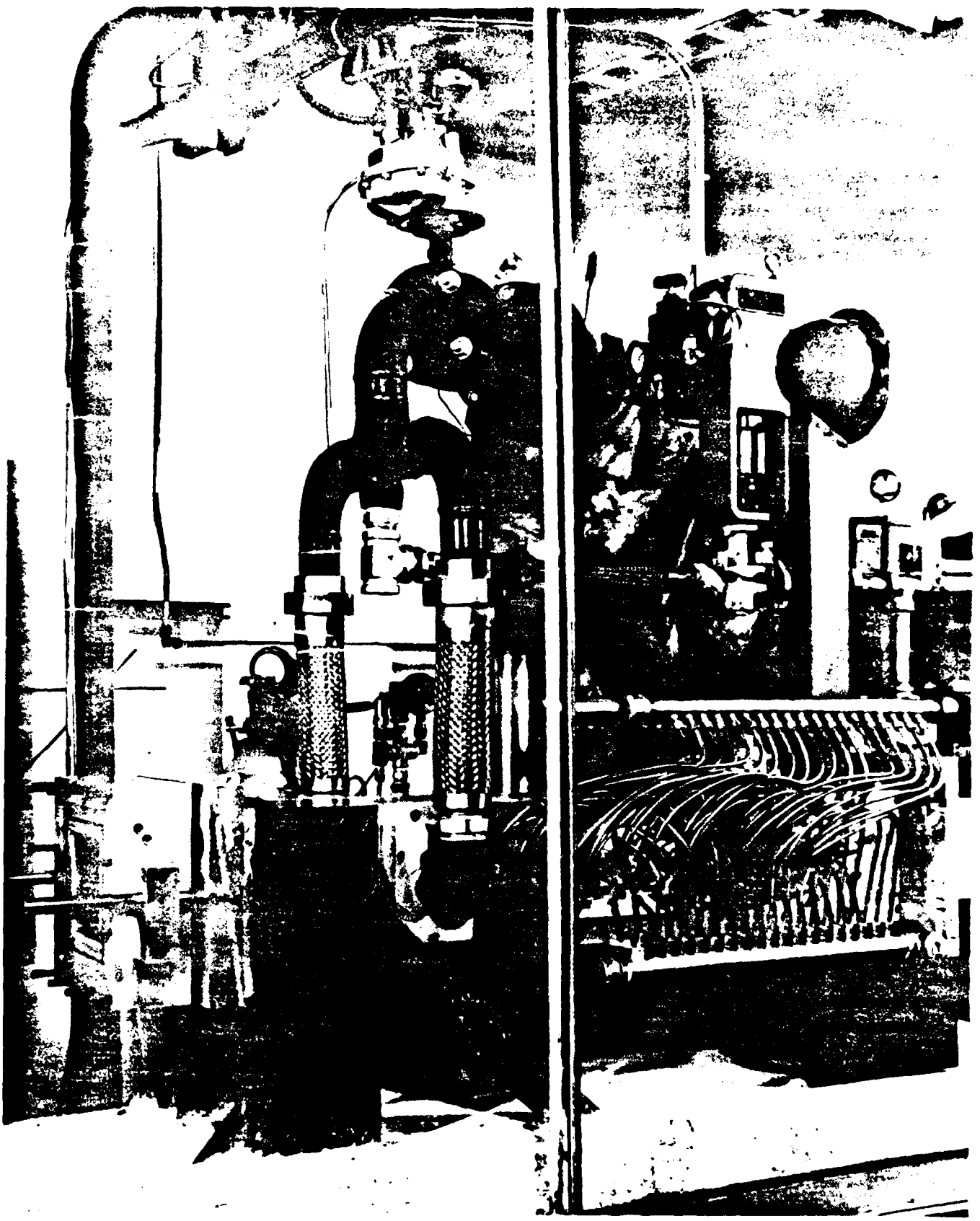

Figure 3. Close-up of Injector Section with Air and Water Supply Plumbing.

driven regions is shared by two diaphragms which are separated by a small gas volume. This pressurized, inter-diaphragm volume is vented to atmosphere at the moment that diaphragm burst is desired, causing the subsequent rupture of the upstream and downstream diaphragms. This will be accomplished by triggering the opening of a fast solenoid value by a timed output signal from the minicomputer after the test section has been filled with droplet/gas mixture. This technique will allow accurate setting of the test pressure in the driver section and good control of the test initiation.

Air/liquid mixtures with mass ratios up to 1.0 will be used in testing. Droplets in the 10-80 μm diameter range will be suspended uniformly throughout the 4.8 meter long test section during planned tests. Relatively high flow rates of both gas and liquid are required in order to provide this medium throughout the test section yet limit the residence time of the mixture to minimize droplet agglomeration and gravitational separation. The flow velocity of 100 msec is provided by gas and liquid streams which enter the driven section through gas and droplet injectors located in a new injector section downstream of the shock tube diaphragms. Most of the gas is injected through sonic nozzles in the injector section sidewalls just downstream of the diaphragm station. This gas flows through the two large pipes which are connected by flexible couplings to distribution manifolds on the injector section sidewalls, as may be seen in Figures 2 and 3. All of the liquid and 13 percent of the gas is injected through up to 80 pneumatic atomizing nozzles which are located downstream of the air injector region. Supply lines to 18 spray nozzles are visible in Figure 3. These tubes are connected to log manifolds above and below the injector section which supply air and water, respectively, to each of the 18 nozzles in the two injector section sidewalls. Provisions have been made to add similar sets of atomizing nozzles in the top and bottom injector section walls to double the current liquid injection rate. The spray nozzles are mounted flush with the sidewalls or in sidewall recesses to control the penetration of each spray jet into the primary air flow. The spray

injectors are installed in arrays at 20, 30, and 40 degree angles to the sidewall to uniformly distribute droplets across the entire flow area.

Steady flow of the droplet/gas stream will be established in the second prior to the diaphragm burst by fast start, blowdown gas and liquid supply systems shown in Figure 1. Air from a 1000 gallon pressurized tank flows through a storage heater to establish and maintain uniform temperature conditions. The storage heater is a pressure vessel which is filled with a wire mesh heat storage matrix which contains sufficient energy for one blowdown test. The storage heater has surface heaters, temperature sensors, and controllers to maintain uniform conditions and is insulated, as may be seen in Figures 2 and 3, to minimize thermal nonuniformities. The metal storage matrix within the heater is preheated by blowing lab air through an external resistance heater which provides the desired temperature and then through the matrix prior to each test to provide a uniform test condition. The storage heater is so configured that the outlet gas temperature will not drop more than 0.2 K in a two second blowdown, which is twice the flow duration planned for each test. An actuated 2.5 inch diameter butterfly valve, which is located downstream of the gas heater, is used to start and stop the gas flow. This valve fully opens in a few tenths of a second to establish steady flow throughout the test section in one second.

Water is injected from a 2 gallon reservoir by displacement using a pressurized gas supply. The water supply reservoir and flow lines will have surface heating installed and will be actively temperature-controlled for later elevated temperature tests. Initial tests will be conducted at ambient liquid temperature conditions. A fast solenoid valving system is used to establish steady liquid flow into the test section within a few tenths of a second after starting the pre-test sequence. The droplet/gas mixture flows from the injector section through the test section to a dump tank, exhaust pipe, and muffler and is exhausted to atmosphere.

Valves which start and stop the gas and liquid flows are controlled by output signals from a PDP-11 based minicomputer system located in the control room. Flow of droplets and gas through the test section will be initiated approximately 1 second prior to diaphragm burst to ensure that this region is entirely filled with a uniform medium prior to shock passage. The diaphragm burst is controlled by a solenoid valve which is used to exhaust gas from between the two diaphragms of the shock tube end. Timing of all flow and data acquisition functions is specified in the minicomputer program which controls testing. Minicomputer subroutines for operating the flow and shock tube controls and taking data during tests are now largely complete.

Assembly and installation of the test apparatus in the laboratory has been largely completed. Most of the plumbing and electrical controls for the shock tube driver and test section have been installed and operationally checked. The task of fabricating and installing air purged windows in the test section for light scattering measurements remains to be completed. These tasks are expected to be completed soon after receipt of the second contract year funding.

Section 3
DIAGNOSTICS

The optical diagnostic which is being used to measure the water droplet size distribution as a function of time is based upon the diffraction of light by groups of individual droplets. A sketch of the hardware used in this technique is shown in Figure 4. Here a collimated beam of laser light (.6328 μm He-Ne) is directed into the droplet laden test section. For droplet sizes which are much greater than the laser wavelength ($d > 2\ \mu m$), the scattered light intensity is given by diffraction from circular apertures of diameter d. As a result, scattered light exits the droplet laden stream at angles characteristic of the individual droplet sizes. The size distribution of droplets can be determined by measuring the angular distribution of scattered light and "inverting" this data. The primary requirement for using this technique is that the integrated line density of droplets not be so large that multiple scattering is important, i.e., a maximum attenuation of 30 percent.

Once the light emerges from the gas, it is collected by a transform lens which converts angle into radial position at the focal plane of the lens. As a result, all light scattered into a range $\Delta\theta$ in angle is monitored over a range in radial position Δr at the focal plane. A multi-element photo diode array with annular symmetry (32 rings) and very fine spatial resolution is used to monitor the radial distribution of light. The normalized measured light distribution is inverted to determine the droplet size distribution which caused the measured light distribution. The unscattered light (~70% or more of the total) is focused tightly on a circular control element so that the unscattered intensity in the presence of droplets can be compared with the intensity with no droplets (hence, no scattering) to determine the attenuation in the presence of scattering. Knowledge of both the attenuation and the size distribution is sufficient to evaluate absolute numbers of droplets

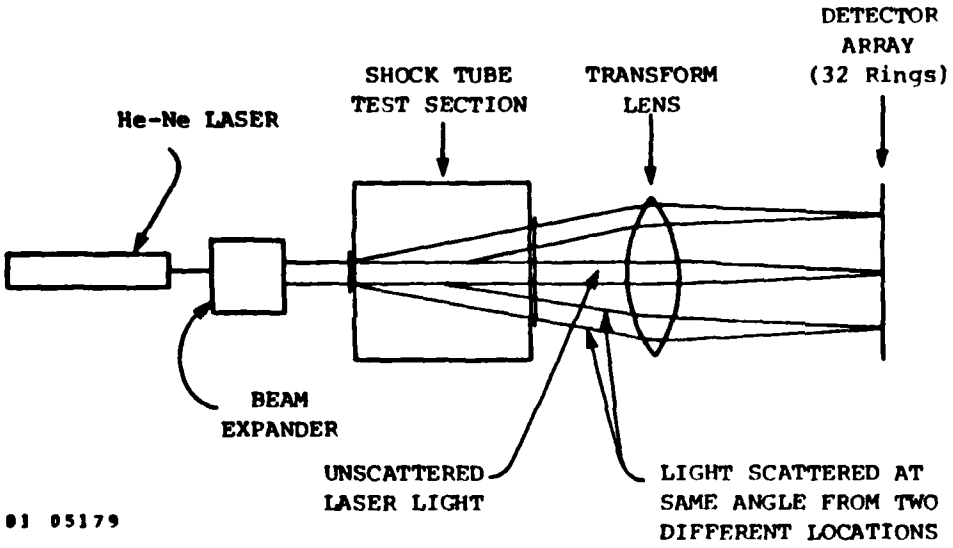

(a) Schematic Diagram of Droplet Light Scattering Diagnostic

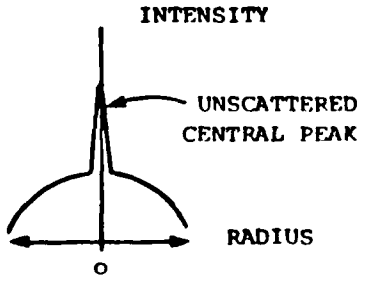

(b) Light Distribution at Detector Array

Figure 4.

in all size ranges. This light scattering technique is very much like that developed by Swithenbank[1] and by Alger[2] for determination of steady droplet size distribution.

A commercial instrument which can automatically do slow droplet sizing measurements like those described above is available for ~$40,000. An evaluation of this instrument was made relative to requirements of the pressure wave suppression tests which we will be doing. This instrument was developed for making steady-state measurements and did not have sufficient time resolution to allow us to follow (without major modification) the rapid changes in size distribution expected after shock passage. Modifying this instrument to have the necessary response and data storage appeared feasible to us, but was not of interest to the manufacturer. Necessary components would have added $10-15,000 to the instrument price and clearly was not possible within the contract funding. Efforts to acquire those parts of this instrument which we would need and to acquire only the software needed to invert the scattered light signal were rejected by the manufacturer (Malvern Instruments). Therefore, we are using the basic scattering techniques mentioned above and have developed a diagnostic package which enables us to make transient droplet size distribution measurements at the required rate.

The analysis technique which is being used to determine the size distribution of droplets from the scattered light intensity distribution was developed at Lawrence Livermore Laboratory and is based on near forward scattering of a collimated, monochromatic light beam by small droplets.[10] The computer code which we have acquired and have made operational on MSNW's VAX 11-780 computer is applicable for polydisperse fields of droplets with a wide range of diameters. Mie scattering theory is used for droplets with diameters comparable to and less than the probe beam wavelength. A diffraction approximation of the Mie theory is used when the droplet diameter is much greater than the probe beam wavelength, as is the case for the droplets expected in the planned tests.

To determine the droplet size distribution from the measured light scattering data, the code uses a number of assumed narrow band droplet size distribution functions. Each of these functions postulates a size distribution of droplets over a small range of droplet sizes, with the full series of functions covering the range of particle sizes expected in the experiment. This would be in the range of ~2 μm to ~80 μm diameter for test conditions after shock passage and ~10 μm to 80 μm prior to shock passage. The chosen narrow band functions overlap each other and are added together in a weighted manner so that the calculated light distribution resulting from the sum of the light distributions from each individual distribution of droplets gives the best fit to the experimental data. The weighting of each of the narrow band functions is determined in an optimization subroutine in the code. The weight addition of the series of size distribution functions then gives the overall droplet size distribution.

While several different individual narrow band functional forms, different numbers of functions, and degrees of overlap could be chosen, our choices to date have been based upon the experience at Lawrence Livermore. Five to eight functions are used with a functional form as follows:

$$f(\alpha) = C(\alpha-\alpha_o)\exp\{-[(\alpha-\alpha_o)/S]^3\}$$

where α is the droplet size parameter $\pi d/\lambda$, α_o is the minimum size parameter which a given narrow band function is assumed to describe, and S is given by $S = (\bar{\alpha}-\alpha_o)3^{1/3}$ where $\bar{\alpha}$ is the assumed mean value of α for the particular narrow band function and C is a normalization constant. The functional form was originally taken from Reference 11. This analysis code has been used to evaluate steady state droplet size distributions using a photographic technique for determining the angular distribution of scattered light.[10] Modifications to the code to operate with the particular optics and detector array of the test have been made, and verification of the code has been completed.

We have purchased an annular detector array and have built amplifiers and buffers that will allow a direct connection to an existing eight channel fast transient digitizer and data storage unit with 32000 words of data storage in our minicomputer data acquisition system. The data time resolution is such that we can determine the complete size distribution every 40 μsec during an experiment. An additional eight channel transient digitizer and memory module will have to be acquired to complete the sixteen parallel channel requirement for scattered light measurements. Recorded data from the detector array will be processed by computer after each test to determine the temporal history of the droplet field following pressure disturbance passage. This system provides the unique capabilities required to study the liquid spray dynamics in a rapidly varying pressure field.

The optical diagnostic system which will be used to measure water droplet size distribution during pressure wave attenuation tests has been assembled and tested in bench top situations. This system is made up of an 8 mw He-Ne laser, a beam expander, a focusing lens, and the photodetector array indicated in Figure 5. An iris, not shown, is used to remove the outer portions of the expanded beam to limit beam size in the scattering medium. These components are mounted on magnetic bases and translators to allow alignment and focusing of the unscattered central portion of the probe laser beam onto the central photodetector spot. This light scattering diagnostic will be mounted on a vibration isolated rail which can be moved to the three window locations in the test section and will not be affected by mechanical vibrations associated with shock tube operation. Data from the photodetector array is coupled through amplifiers to fast transient digitizers and stored in digitizer memory modules during each test. This unique, fast light scattering diagnostic is described in greater detail below.

The photodetector array consists of thirty two concentric annular rings, as shown in Figure 5. The ring area increases with radial position from the central spot, as indicated in Table 1. Sixteen pairs of adjacent

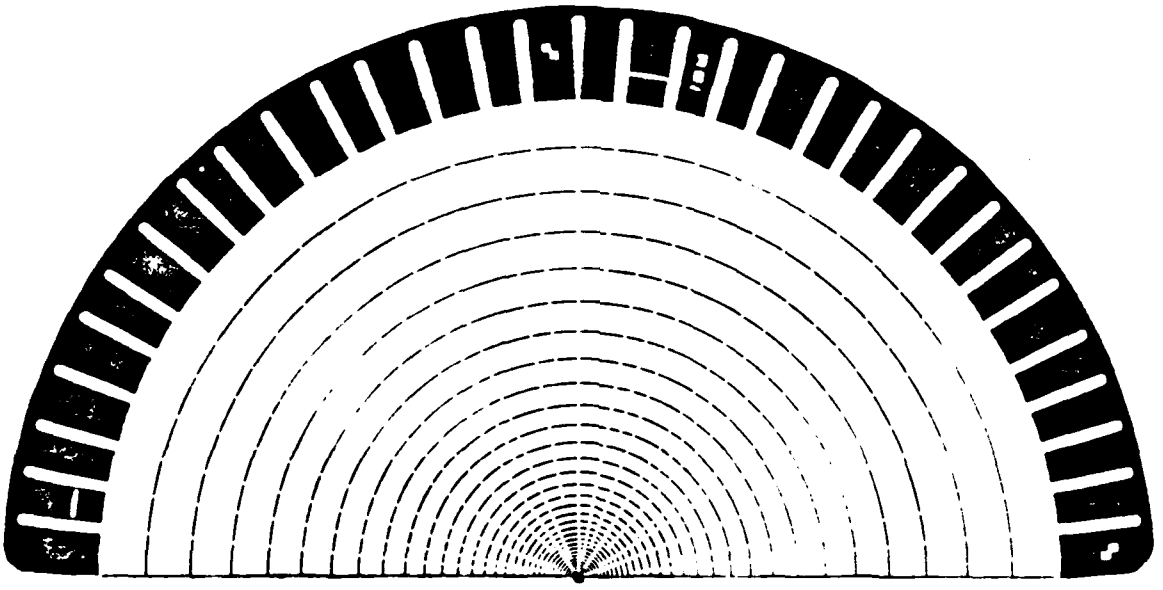

Figure 5. Configuration of Thirty Two Element Photodetector Array.

Table 1

Dimensions of Photodetector Array

Ring Number	Outer Radius (mils)	Area	
		Sq. mils	Sq. cms
1	3.5	38.48	2.483×10^{-4}
2	8.6	43.46	2.80
3	12.5	69.14	4.47
4	16.4	93.53	6.05
5	20.4	122.70	7.94
6	24.6	148.62	9.60
7	29.0	189.99	1.225×10^{-3}
8	33.7	244.95	1.58
9	38.8	318.67	2.30
10	44.4	417.39	2.70
11	50.6	548.70	3.55
12	57.5	721.98	4.67
13	65.2	948.69	6.12
14	74.0	1279.58	8.26
15	83.9	1688.83	1.09×10^{-2}
16	95.1	2236.98	1.445
17	107.8	2963.58	1.92
18	122.1	3884.69	2.51
19	138.3	5114.32	3.29
20	156.6	6697.14	4.34
21	177.2	8715.36	5.62
22	200.2	11209.04	7.24
23	225.9	14385.46	9.27
24	254.7	18473.35	1.195×10^{-1}
25	286.7	23448.54	1.515
26	322.2	29630.12	1.92
27	361.6	37361.62	2.41
28	405.0	46614.09	3.01
29	452.8	57987.95	3.74
30	505.4	71889.37	4.65
31	563.0	88448.67	5.71
32	626.0	108409.80	7.00×10^{-1}

detector rings are being used to define the angular distribution and provide sufficient data to accurately define the droplet size distribution during transient tests. Amplifiers have been developed for each channel to provide the gain and bandwidth required to give a nominally full scale signal to each of sixteen transient digitizer channels when the detector sees the expected maximum scattered light intensity to maximize accuracy. The expected light intensity distributions have been calculated by using the scattering computer routine which is used in data reduction along with expected particle size distributions and has been confirmed, in part, through steady flow scattering tests with droplet streams. The frequency response of each detector-amplifier circuit has been maintained at ~100 kHz to resolve the transient droplet dynamics following wave passage. The design gains in the range of 1 to almost 1000 and bandwidth for at least 100 kHz frequency response for each amplifier-photodetector circuit have been confirmed by monitoring outputs while inputing a rapidly pulsed light source to each pair of photodetector rings. Thus, the photodetector diagnostic is now known to have adequate response and stability to measure changes in angular distribution due to flow transients at rates up to ~100 kHz. The actual sampling rate will be limited to 40 kHz by the digitizing rates of the two Lecroy 2264 transient digitizers and memory modules which will be used to acquire and store the scattered light data during tests.

Several small problems were found during the initial tests of the light scattering diagnostic. A small fraction of the focused probe laser beam reflects from the front surface of the detector array back toward the light source. Reflection of this light from the focusing lens back onto the outer rings of the detector was of the order of the scattered light intensity when uncoated optics were used. To eliminate this problem, the focusing lens has been anti-reflection coated at the He-Ne wavelength. Reflections are no longer a problem. The two outer rings of the detector which gave anomalously low readings during early tests and appeared to be defective have been operating normally since new connections were made at the detector board. These and other small problems found during earlier checkout tests have been largely resolved.

We have completed bench measurements of the scattered light from a single, free-standing water jet nozzle. Measured data is plotted as intensity versus scattering angle in Figure 6. The intensity is in arbitrary units and was calculated by taking the measured voltage for each pair of rings (the voltage is directly proportional to the amount of light) and dividing by the sum of the surface area of each ring of a given pair. The light scattering code was then used to determine from the intensity versus angle data the relative number distribution of particles versus particle size parameter $\alpha(= \pi d/\lambda$ where d is diameter and λ is scattered light wavelength). The results obtained using the data given in Figure 6 are shown in Figure 7. The latter results indicate that the number distribution of the jet droplets is strongly peaked at $\alpha \cong 195$. This is consistent with information given us by the nozzle manufacturer. (The negative values for $n(\alpha)$ are associated with an instability in the optimization routine and are thought to be numerically insignificant.) There is, however, significant sensitivity to the input data, especially in the high intensity central region. Ten percent variations in the input data can cause secondary peaks to arise in the derived distribution and can cause the location of the main peak to shift substantially. This is exemplified by the dashed line in Figure 7 for a case where the data point at the smallest angle was decreased by ten percent. We are continuing to examine this problem and its implications, as well as those resulting from the small negative values for $N(\alpha)$.

Substantially greater quantities of data will be available early in the second program year when the scattering diagnostic is fully automated. Several improvements in the data analysis code will be made to make its operation with test data more accurate and consistent. First, the code will be modified to deal with the actual radial distribution of light at the sensor ring locations. At present, the use of uniformly spaced radial locations requires that the data be curve fit prior to reduction and that intensity be interpolated between measured locations, resulting in some error. Another change that will be analyzed will be to base the data reduction on measured light energy per unit radius as used

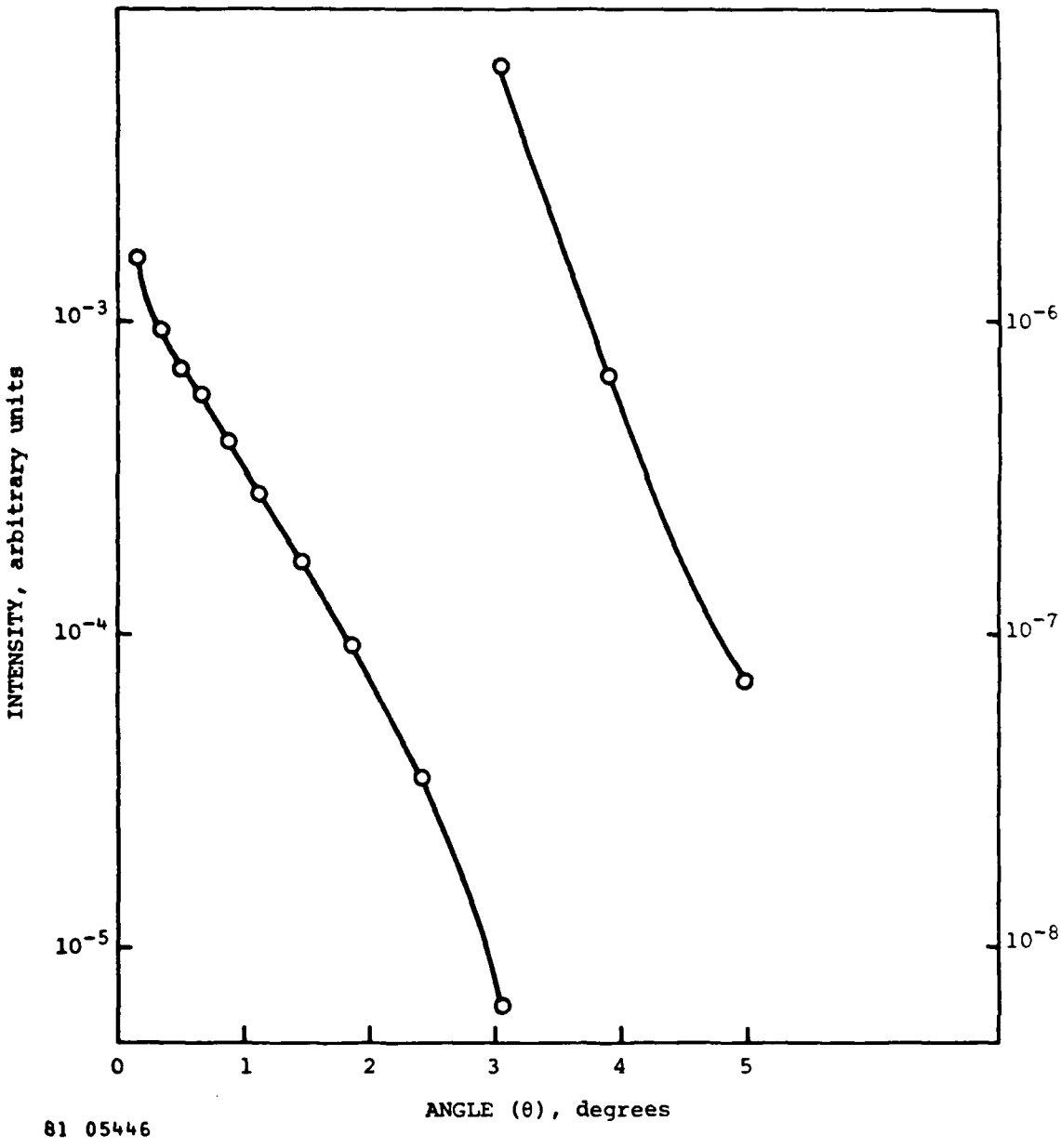

Figure 6. Scattered Light Data from Single Jet Atomizing Nozzle.

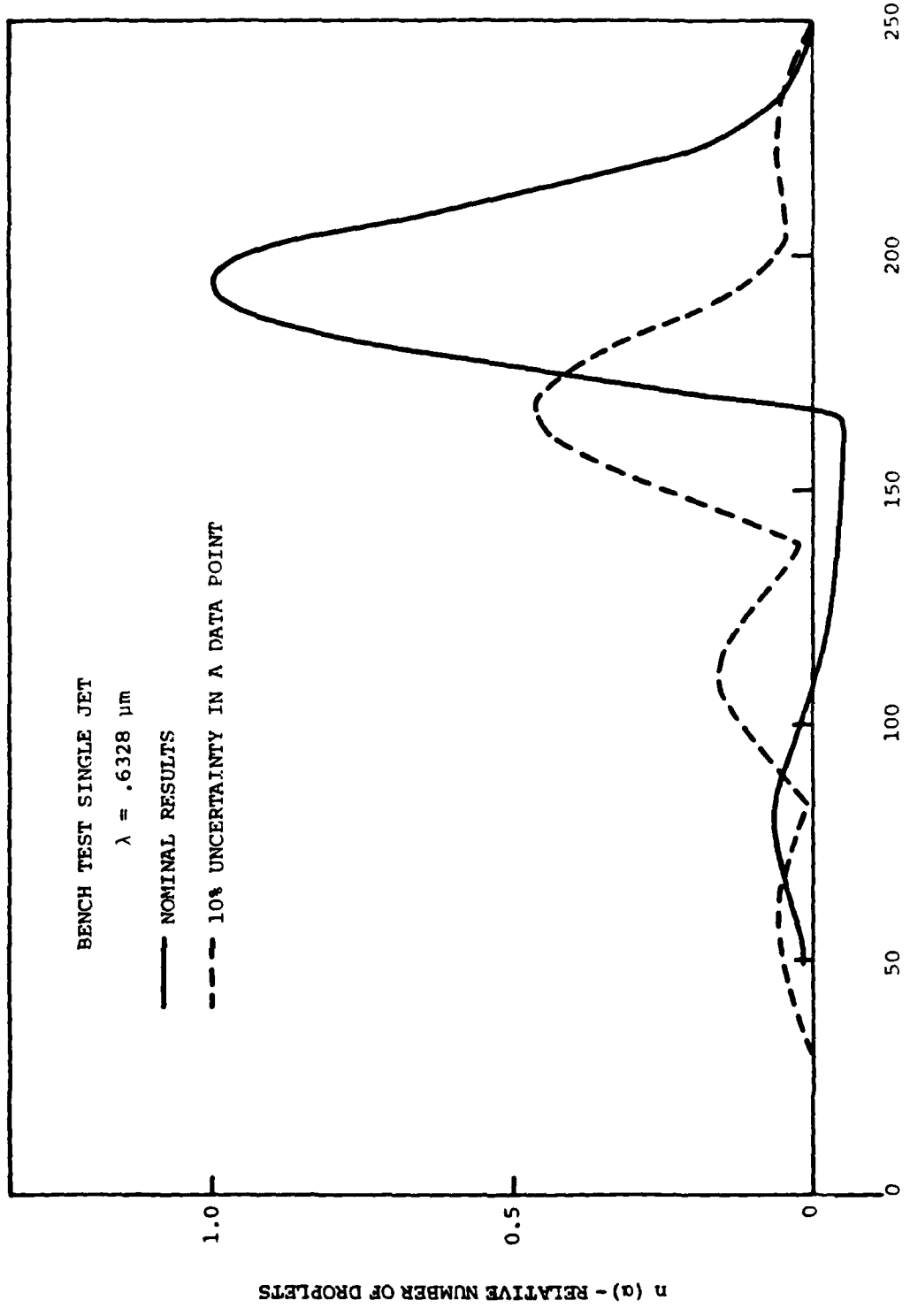

Figure 7. Computed Droplet Size Distributions for Single Jet Atomizing Nozzle.

by Swithenbank[9] rather than light per unit area (intensity) as currently used. It is expected that the Swithenbank technique will lessen the sensitivity of the calculated droplet size distribution to small variations of input data near the center detector element. Additional experience in the use of various numbers and widths of narrow band droplet distribution functions is expected to provide more rapid and stable convergence to an optimum size distribution profile. These changes in the code and the way the code is used are straightforward and are expected to improve the stability and accuracy of droplet size distributions calculated from test data.

Other diagnostic equipment such as pressure transducers, pressure gauges, gas analysis, thermocouples, and flow meters have been selected for monitoring shock tube fill conditions, test section steady flow conditions, and dynamic pressure variations. Shock tube fill pressures will be monitored using 0.25 percent accurate pressure gauges. Gas composition will be monitored using an existing gas sampling system and gas chromatograph. Steady flow conditions to the test section will be monitored using thermocouple probes, standard ASME flow nozzles in the inlet lines, and strain gauge pressure transducers. Dynamic pressures will be measured at four axial stations in the test section using PCB Model 112A21 high resolution pressure transducers. Equipment, techniques, and software are operational for calibration, use, and reduction of data from these instruments in dynamic tests as controlled by the laboratory's PDP-11 based minicomputer system.

REFERENCES

1. Thayer, W.J. et al., "Pressure Wave Suppression for a Pulsed Chemical Laser," AIAA Journal, Volume 18, No. 6, pp. 657-664, 1980.

2. Buonadonna, V.R. et al., "Performance Characteristics of a Wave Attenuator for Pulsed Chemical Lasers," AIAA Paper 81-1284, 14th Fluid and Plasmadynamics Conference, Palo Alto, California, June 1981.

3. Reineke, W.G. and Waldman, G.D., "Shock Layer Shattering of Cloud Drops of Re-entry Flight," AIAA Paper 75-152, January 1975.

4. Simpkins, P.G. and Babes, E.L., "Water Drop Response to Sudden Accelerations," Journal of Fluid Mechanics, Volume 55, No. 4, pp. 629-639, 1972.

5. Ranger, A.A., "Shock Wave Propagation Through a Two-Phase Medium," Astronautica Acta, Volume 17, pp. 675-683, 1969.

6. Marble, F.E., "Some Gasdynamic Problems In The Plow of Condensing Vapors," Astronautica Acta, Volume 14, pp. 585-614, 1969.

7. Marble, F.E. and Candel, S.M., "Acoustic Attenuation in Fans and Ducts by Vaporization of Liquid Droplets," AIAA Journal, Volume 13, No. 5, pp. 634-639, 1975.

8. Lyman, F.A. and Chen, D.M., "Acoustic Attenuation in a Nonuniform Gas Containing Droplets," AIAA Journal, Volume 16, No. 5, pp. 503-509, 1978.

9. Swithenbank, J. et al., "A Laser Technique for the Measurement of Droplet and Particle Size Distribution," Experimental Diagnostics in

Gas Phase Combustion Systems, Progress in Aeronautics and Astronautics, Volume 53, B.T. Zim, Editor, 1977.

10. Alger, T.W., "Polydisperse-Particle-Size-Distribution Function Determined from Intensity Profile of Angularly Scattered Light," Applied Optics, Volume 18, No. 2-, p. 3494, October 1979.

11. Korker, M., The Scattering of Light and Other Electromagnetic Radiation, Academic Press, New York, 1969.


FILMED
5-8